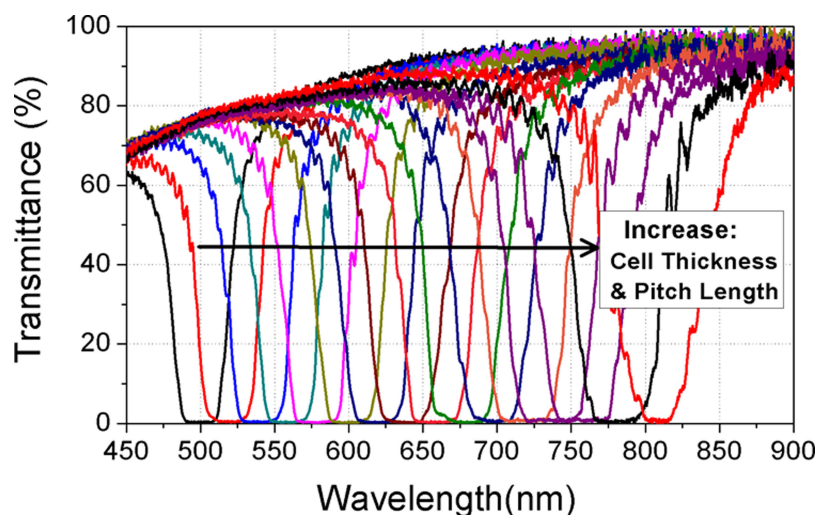


Continuously Tunable and Bandwidth Variable Optical Notch/Band-Pass Filters Over 500 nm Spectral Range Using Cholesteric Liquid Crystals

Volume 11, Number 1, February 2019

Mi-Yun Jeong
Keumcheol Kwak



Spectra of the continuous tunable notch filter system by wedge CLC cells.

Continuously Tunable and Bandwidth Variable Optical Notch/Band-Pass Filters Over 500 nm Spectral Range Using Cholesteric Liquid Crystals

Mi-Yun Jeong ¹ and Keumcheol Kwak ²

¹Department of Physics and Research Institute of Natural Science, Gyeongsang National University, Jinju 52828, South Korea

²School of Electronics and Electrical Engineering, Sungkyunkwan University, Suwon 16419, South Korea

DOI:10.1109/JPHOT.2018.2884965

1943-0655 © 2018 IEEE. Translations and content mining are permitted for academic research only. Personal use is also permitted, but republication/redistribution requires IEEE permission. See http://www.ieee.org/publications_standards/publications/rights/index.html for more information.

Manuscript received October 29, 2018; revised November 28, 2018; accepted November 29, 2018. Date of publication December 4, 2018; date of current version December 28, 2018. This work was supported in part by the Basic Science Research Program through the National Research Foundation of Korea (NRF), in part by the Ministry of Science, ICT & Future Planning (2017R1D1A1A02019309), and in part by the Development Fund Foundation, Gyeongsang National University, 2018. Corresponding author: Mi-Yun Jeong (email: jmy97@gnu.ac.kr).

Abstract: We report continuously tunable and bandwidth variable optical notch and band-pass filters created by combining four left- and right-handed circular cholesteric liquid crystal cells without extra optical components. Filter performance was greatly improved by introducing an anti-reflection layer on the filter device. The filter comprised cholesteric liquid crystal wedge cells with continuous pitch gradient. The band wavelength position was spatially tuned from 470 nm to 1000 nm. The notch filters are polarization-independent in the spectral ranges. The band pass filters can be designed to be polarization-independent or polarization-dependent via cell alignment and the bandwidth can be reversibly controlled from the original bandwidth (60~18 nm). These tunable filter strategies could make a paved road to wavelength tunable spectroscopic instruments applications in the VIS and near infrared response spectral range.

Index Terms: Optical devices, optical filter, liquid crystal devices, photonic crystal filter.

1. Introduction

Optical notch and band-pass filters are fundamental and essential devices for selectively manipulating the wavelength of light in optical signal processing applications, such as imaging Raman spectroscopy, multi-photon microscopy, laser-based fluorescence, astronomical telescopes, and supercontinuum. Optical filters are currently one of the indispensable devices in satisfying the acute need for massive and high-speed communication, and to implement optical wavelength division multiplexing (WDM) and orthogonal frequency division multiplexing (OFDM) systems in optical communication systems [1]–[3]. In addition, optical filters are required to provide independent and continuous tuning of both wavelength and bandwidth to cater to the flexible spectral arrangement [4]–[6]. Up to now, in order to control optical band structure and transmission properties of optical devices some excellent strategies with different optical characteristics have been studied, including the microelectromechanical system (MEMS) [7], Fabry-Perot interferometer tunable

filters [8], acousto-optic tunable filters, electro-optical filters [9], [10], and metallodielectric photonic crystal systems [11]–[14], etc. In recent years, due to multi-functional capability, various phases of liquid crystals (LCs) have been widely applied to develop tunable filters [15]–[26], tunable laser devices [27]–[31], reflective color display devices [32]–[33], and tunable photodetectors [34], etc. Among them, cholesteric liquid crystals (CLCs) consist of nematic liquid crystals (NLCs) and chiral molecules and have self-organized periodic helical nano structures. Especially, the benefits of CLCs include the ability to control the photonic band gap (PBG, Bragg reflection) width and its spectral position by, for example, adjusting the birefringence of the NLC (n_o and n_e), chiral dopant concentration [27], temperature control [28], UV curing [35]–[36], and application of an electric field [37].

In a previous study, we reported a continuously tunable optical notch and band-pass filter system that covers the VIS to NIR spectral range [23], but there was light leakage of $\sim 3\%$ inside the band of the filters, and transmittance outside the band was low, from 70% to 40%. To apply this system as a practical filter device, a prerequisite is solving the light leakage in the band. Going one step further would be to increase the transmission rate outside of the band. Thus, to solve the problems with the filter, in this paper, we present two strategies in the current paper: the introduction of an anti-reflection coating layer (AR-layer) between the air and substrate BK7 interface of the CLC cell structure and the application of multiple cell reflection by combining two CLC cells with left-handed helicity (L-CLC) and two CLC cells with right-handed helicity (R-CLC). We introduced two continuous wavelength tunable filters over a 500-nm spectral range; the first one is an optical notch filter with pitch gradient and the second one is an optical band-pass filter with pitch gradient whose bandwidth could be reversibly variable from the original bandwidth of ~ 60 nm to ~ 18 nm without light leakage in the band. And the transmittance outside of the band is 70~100%. To the best of our knowledge, continuous tunable and bandwidth variable filter without extra optical components over a 500-nm spectral range with independent wavelength position and have high performance has not been previously developed. These multi-functional filters could be widely utilized in various optical instruments.

2. Optical Properties of CLC Filters

CLCs consist of nematic liquid crystals (NLCs) and chiral molecules and have self-organized periodic helical nano structures. Fig. 1(a) shows that for circularly polarized light with the same handedness as CLCs, selective (Bragg) reflection occurs in the wavelength range, $n_o P < \lambda < n_e P$ with photonic bandwidth $(|n_e - n_o| \times P)$, where the pitch (P) is the length for one full rotation of the director around the helix axis and is determined by the concentration of chiral molecules. n_o and n_e are the ordinary and extraordinary refractive indices of the nematic molecules, respectively [23], [27], [38]. Fig. 1(b) shows principle of a notch filter by a CLC with left handed helix (L-CLC) and a CLC with right handed helix (R-CLC). For unpolarized incident light, left circularly polarized light in the band is reflected at the CLC with left handed helix and right circularly polarized light in the band is reflected at the CLC with right handed helix, in turn.

Fig. 2 shows a fabricated CLC wedge cell structure with pitch gradient by PI/BK7/AR substrates. The cholesteric helical pitches were quantized with the number of half- turns [38] by the boundary condition. Along the positive x -direction, a linear increase of the helical pitch (P) continuously took place. This continuous tuning behavior is due to the fact that the concentration of pitch gradient matches the fixed helical pitch determined by the cell thickness [39]. Therefore, spatially, the wavelength position of PBG ($n_o P < \lambda < n_e P$) also continuously changes according to the pitch change along the x -direction on the CLC cell. A method to fabricate the CLC wedge cell structure with pitch gradient is given in the Section 3. Experimental Details.

3. Experimental Details

In order to study a continuously tunable filter system with high performance, we fabricated CLC cells which had a pitch gradient by changing the chiral molecular concentration along the wedge

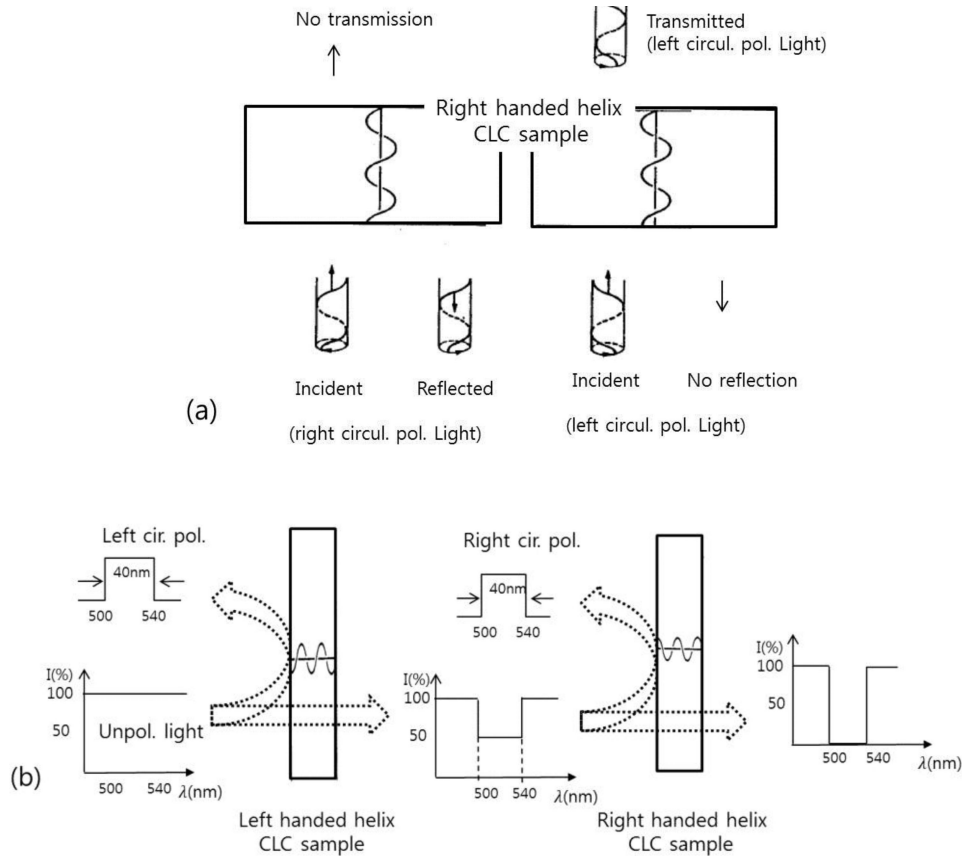


Fig. 1. (a) Bragg reflection and transmission by a planar CLC cell with right handed helix. (b) Principle of a notch filter: for unpolarized incident light, left circularly polarized light in the band is reflected at the CLC with left handed helix and right circularly polarized light in the band is reflected at the CLC with right handed helix, in turn.

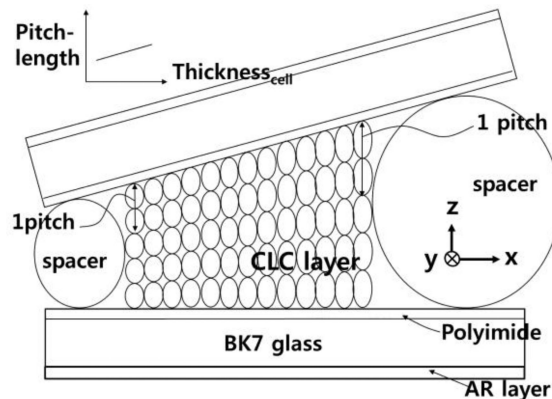
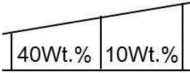
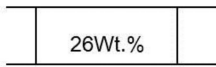


Fig. 2. Schematic diagram of the wedge CLC cell with pitch gradient.

cell. And to study the effect of antireflection (AR) coating layer on substrate (BK7) and the difference of three kind substrates, we also made the three kinds of parallel CLC cells with different substrates those had no pitch gradient and had one chiral molecular concentration. There are several steps to making CLC cells. As a substrate, we used three kinds of plates: BK7 plates, BK7 plates with one side coated with an antireflection(AR)-layer for spectral range from 400 nm to 1000 nm ($0.6 \mu\text{m}$

TABLE 1
The Fabrication Process of the CLC Cells

Preparation Process Order	Wedge CLC Cell	Parallel CLC Cell
1. AR coating (400nm~1000nm)	BK7/AR	BK7/AR
2. PI-spin coating and rubbing	PI/BK7/AR	PI/BK7, PI/BK7/AR, PI/ITO/Glass
3. Empty cell fabrication	AR/BK7/PI/Air/PI/BK7/AR-layer Ball space (30 μm , 40 μm)	AR/BK7/PI/Air/PI/BK7/AR BK7/PI/Air/PI/BK7 Glass/ITO/PI/Air/PI/ITO/Glass Ball space (30 μm , 10 μm)
4. CLC Mixing: L-CLC: MLC6608+S811 R-CLC: MLC6608+R811	L-CLC: 10Wt.%, 40Wt.% R-CLC: 10Wt.%, 40Wt.%	L-CLC: 26Wt.%
5. Inject CLCs in to the cells		
6. Development time: for pitch gradient	For ~5 weeks	No pitch gradient
7. Number of cells	L-CLC cell: 2 ea R-CLC cell: 2 ea	L-CLC cells with 3 different plates : 3 ea

thickness, Yunam Optics, Inc., Korea), and glass plates with one side coated with an indium tin oxide (ITO) layer. On the surface of each plate, a polyimide (PI) (SE-5291, pretilt angle of $6^\circ \sim 7^\circ$, Nissan Chemical Korea Co. Ltd., Korea) layer is spin coated, resulting in the fabrication of three kinds of multilayer substrates: PI/BK7, PI/BK7/AR-layer, and PI/ITO/glass. After the PI coating, the plates were thermally treated to crosslink PI, and then the PI layers were rubbed with a rubbing cloth (HC20, cotton, NESTECHNOLOGY Co., Ltd, Korea). With the PI-coated surface facing inward, empty wedge cells were fabricated by employing spacers of two different sizes (thin: 30 μm , thick: 40 μm) with a lateral distance of ~ 2.6 cm. The L-CLC and R-CLC cells were made by mixing a nematic LC, MLC6608 with negative dielectric anisotropy and two chiral dopants, S811 for left-handed helicity and R811 for right-handed helicity (all from Merck, Korea). Because the MLC6608 is one of the smallest birefringent nematic liquid crystals, it was selected to make the filters having narrow photonic bandwidth ($|n_e - n_o| \times P$). In order to cover the VIS and NIR spectral range, chiral dopant concentrations of L-CLCs and R-CLCs were selected as 10 Wt.% and 40 Wt.%. The L-CLCs and R-CLCs with low, ~ 10 Wt.% chiral dopant concentrations were half-filled at the thick spacer position of each empty wedge cell, and then those with high, ~ 40 Wt.% chiral dopant concentrations were half-filled at the thin spacer position. To develop a chiral dopant concentration gradient along the wedge direction through the chiral dopant diffusion of the helical rotatory power, the CLC-filled cells were kept at room temperature for ~ 5 weeks. The fabricating process of the CLC cells is summarized in the Table 1. Fig. 3 shows the fabricated CLC cells: two R-CLC (Figs. 3(a) and (b)) and two L-CLC (Figs. 3(c) and (d)) wedge cells using PI/BK7/AR-layer plates (~ 22 mm \times 45 mm \times 1 mm) with a pitch gradient, and three parallel L-CLC cells with S811 (26 Wt.%); a 30 μm thick L-CLC cell (~ 22 mm \times 45 mm \times 1 mm) using PI/BK7/AR-layer plates (3e), a 10 μm thick L-CLC cell (~ 18 mm \times 25 mm \times 1 mm) with PI/BK7 plates (3f), and a 10 μm thick L-CLC cell (~ 18 mm \times 25 mm \times 1 mm) with PI/ITO/glass plates (3g), respectively. Even though the same L-CLC (S811, 26 Wt.%) is in three cells (e, f, and g), the reflection color is a little bit different due to the difference in transmittance (or reflectance) by the different substrates of the cells (see Figs. 3 and 4). The benefit of the CLC cells with the single concentration (26 Wt%) is that they do not need a long

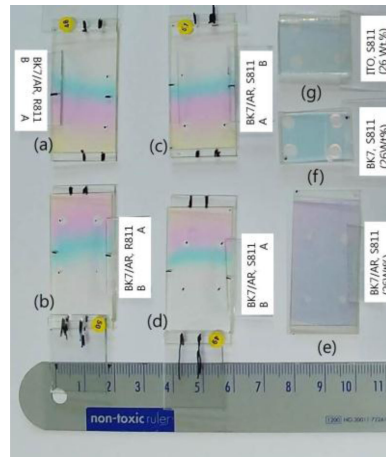


Fig. 3. Fabricated wedge R-CLC cells (a and b) and L-CLC cells (c and d) using PI/BK7/AR substrates with a pitch gradient and three parallel L-CLC cells using PI/BK7/AR (e), PI/ITO/glass plates (f), and PI/BK7 plates (g), respectively.

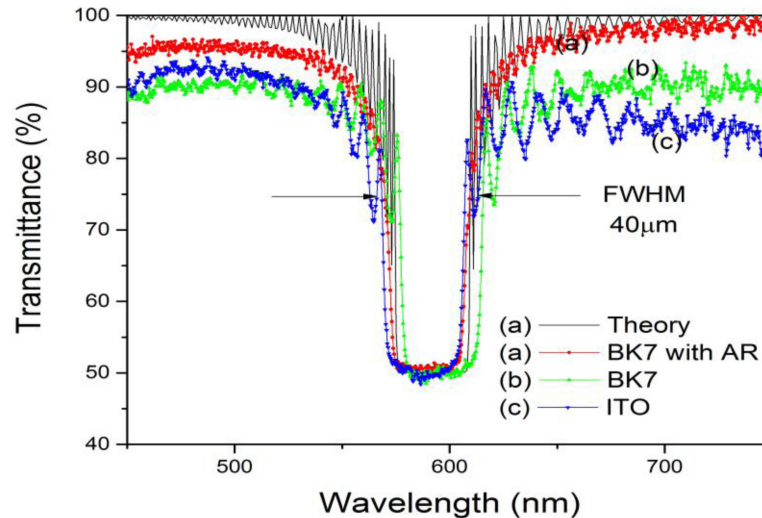


Fig. 4. Transmittance of the PBGs of L-CLC cells (S811, 26 Wt.%). (a) PI/BK7/AR-layer plates. (b) PI/BK7 plates. (c) PI/ITO/glass plates. Solid line is theoretical fitting data of (a).

period of time to form a CLC pitch. The transmitted spectrum from the CLC cells and band-pass filter and notch filter were measured by a spectrometer with a resolution of 0.36 nm (HR 2000+, Ocean Optics, and USA).

4. Results and Discussion

Fig. 4 shows the transmittances of 50% by the selective (Bragg) reflection of three parallel CLC cells with the same L-CLC material but different substrates using the PI/BK7/AR-layer plates (Fig. 4(a), 30 μm thickness cell), PI/BK7 plates (Fig. 4(b), 10 μm), and PI/ITO/glass plates (Fig. 4(c), 10 μm). And solid line of the Fig. 4(a) is theoretical fitting using Berreman's 4×4 matrix method [40]–[42]. The theoretical fitting parameters of Fig. 4(a) with central wavelength of 590.5 nm of the Bragg reflection are as follows: for L-CLC, thickness of 29 μm , ordinary refractive index (n_o) of 1.5252, and extraordinary refractive index (n_e) of 1.6111; for BK7, thickness of 1 mm and refractive index of

1.5129. In the theoretical fitting, the polyimide (PI) layer was ignored. Due to AR-layer on BK7 in the CLC cell structure (Fig. 2), the reflectance at each boundary surface of air/AR-layer/BK7/CLC layers was also ignored. The measured band center position with 590 nm and bandwidth with 40 nm for PBGs were somewhat coincident with theoretical calculations. There is some difference between measured data and theoretically fitted data curves near band edges. The experimentally measured values were gently decreased. However, in theoretically fitted curves, large oscillations occurred near the band edge. And Fig. 4(b) and 4(c) data values from CLC cells with 10 μm thickness, oscillated greatly near band edge. When considering the behavior, it seems that in the theoretical calculations, CLC molecules are assumed to form a perfect helical structure regardless of CLC thickness. However, in a real CLC cell with thin thickness, these molecules could be aligned with the perfect helical structure by cooperation between anchoring force of the alignment layer and helical rotary powers of chiral molecules. Therefore, the transmittance oscillated near the band edge. However, as the film thickness increased, it was harder to form a perfect helical structure due to weak cooperation in the bulk area far from the alignment layer because the helical structure of molecules in the CLC cell originated from the cooperation of the anchoring energy between CLC molecules and the alignment layer (PI) and the helical rotary power of chiral molecules [30]. To apply the CLC cell to a practical filter device, the oscillation near the band edge is a decisive disadvantage. Based on results of this study, an appropriate thickness for the CLC filter would be $\sim 30 \mu\text{m}$.

The transmittance of Fig. 4(a) decreased from 100% to 95% when wavelength was decreased from 600 nm to a short wavelength due to refractive index mismatch that still existed slightly between the air/AR-layer/BK7/PI/CLC layers, although there was AR coating on BK7. Meanwhile, by comparing the transmittances of the three CLC cells, we could determine the efficiency of the AR-layer on BK7 plates and the effect of different substrates on transmittance. Inside the band, near 590 nm, the reflectance of all cells was approximately 50%. However, despite the same L-CLC concentration in each cell, the PBG position of the curve differed by ~ 10 nm (compare Fig. 4(b) to Fig. 4(a) and 4(c)). This difference may satisfy the boundary condition, or the cholesteric helical pitches were quantized by the number of half-turns between two substrates of the cell [28], [38]. Outside the bands, there was large difference in transmittance; the transmittance of the cell without the AR-layer (Fig. 4(b)) was $\sim 90\%$ over the spectral range, whereas the transmittance of the cell with the AR-layer (Fig. 4(a)) was approximately 95% around 450 nm ~ 600 nm and $\sim 100\%$ over the 600-nm spectral range.

The PI/ITO/glass plate is widely used for CLC cell fabrication due to good flatness and its ease with using electrodes [23], [30], [38]. Therefore, we also compared the transmittance of the previous CLC cell; the transmittance outside the band dramatically decreased from 90% to 65% as wavelength increased (Fig. 4(c)). This serious behavior is a result of the refractive index mismatch between neighboring layers of the CLC/PI/ITO/glass/air of the substrate and ITO layer. And the absorption rate of the employed ITO layer is $\sim 2.5\%$ near 550 nm and monotonously increasing over the long wavelengths to around 15% near 1000 nm. In our previous filter devices, similar results were obtained with the notch filter and band-pass filter [23]. Thus, the transmittance is influenced not only by the CLC material, but also the boundary condition of the layers of the cell. As seen in Fig. 4, the AR-layer on the BK7 (or glass) substrate could solve the refractive index mismatch between the air and glass layers of the CLC cell. We can conclude that the AR-layer on the surface of BK7 CLC cells is a vital factor in greatly improving transmittance and solving the light leakage problem in the notch filter. Moreover, near the PBG edge are large oscillations in transmittance (Fig. 4(b) and (c)) when the cell thickness is $\sim 10 \mu\text{m}$. In contrast, no oscillation in transmittance was seen when the cell thickness was $\sim 30 \mu\text{m}$ (Fig. 4(a)). Therefore, to remove unnecessary oscillation near the PBG, the required cell thickness is approximately 30 μm .

Fig. 5 shows two combined experimental setups with the notch filter and band-pass filter system. For the notch filter, a 1-set CLC notch (including an L-CLC [L1 or L2], an R-CLC [R1 or R2], and waveguides of 400- μm diameter [W1]) or 2-set CLC notch (including L1, R1, L2, R2, and W1) were employed. For the band-pass filter, a beam splitter (BS), L1, R1, and W2, or BS, L1, R1' (R-CLC), and a waveguide 400 μm in diameter (W2) were employed. In order to spatially move the PBG

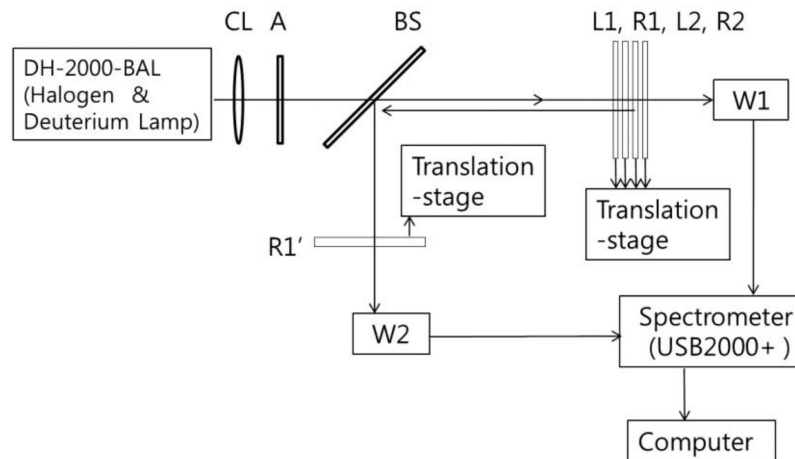


Fig. 5. Experimental set up of the notch filter and band-pass filter system: CL, lens for a collimated beam; A, aperture; BS, beam splitter; L1 and L2, L-CLC cells; R1, R2, and R1', R-CLC cells; and W1 and W2, waveguides of 400 μm diameter. Depending on the purpose of the filter, some L1, L2, R1, R2, and R2' cells could be removed from the setup.

position of the CLC cells, 4 translation stages were employed. Depending on the purpose of the filter, some cells of L1, L2, R1, R2, and R2' could be removed from the setup. The light signal from the filters was acquired through the waveguides by the spectrometer (USB2000+).

Fig. 6(a) shows notch spectra from 470 nm to 960 nm for the different spatial positions of the continuous tunable notch filter system using the AR-layer coated L1 and R1 with a pitch gradient and W1 in Fig. 5, the 1-set notch (N1) system. Data were measured by moving the L1 and R1 with translation stages to maintain the same PBG position. For unpolarized incident light, left circularly polarized light in the band is reflected at L1 and right circularly polarized light in the band is reflected at R1, in turn. Therefore, all of the light in the band is reflected and the light outside the band is transmitted, as shown in Fig. 4(b). The transmittance through W1 is set to 100% when L1 and R1 are removed (Fig. 5). By moving to the lateral thick wedge direction in the cell with a pitch gradient, the PBG shifts to a long wavelength, and the full-width at half maximum (FWHM) of the PBG gradually increases from ~ 33 nm at 480 nm to ~ 60 nm at 970 nm. As the wavelength increases, the transmittance of the outside of the band is increased from 80% near ~ 500 nm to 100% near 900 nm. This value and behavior are a great improvement compared to our previous paper in which the transmittance outside the band was decreased from 70% near 500 nm to 40% near 900 nm [23]. However, inside the band, there was still light leakage of 1~3% across the spectral range, indicating that, although the AR-layer between the air and BK7 improved the reflective index mismatch and interference between the CLC cells. For practical applications, light leakage of 1%~3% in the band is not allowed in a notch filter device. To solve this problem, we applied a multiple cell reflection method using two L-CLC cells (L1 and L2) and two R-CLC cells (R1 and R2) in the 2-set notch (N2) system (Fig. 5). The R1, R2, L1, and L2 cells are wedge cells with a pitch gradient corresponding to Fig. 3(a)-(d), respectively. Fig. 6(b) shows notch spectra from 470 nm to 850 nm using N2 system filters. No light leakage was seen in the band, but outside the band the transmittance was decreased by 2–10%.

Fig. 7(a) shows continuous band spectra from ~ 480 nm to ~ 950 nm from the tunable band-pass filter system consisting of L1, R1, BS, and W2 in Fig. 5. The data were measured by moving the L1 and R1 cells with translation stages to maintain the same PBG position. For unpolarized incident light, left circularly polarized light in the band of L1 and right circularly polarized light in the band of R1 are reflected to the BS by L1 and R1, respectively. All the light in the band is then reflected again from the BS to W2. As all of the light in the band is reflected, this type of band-pass filter system is polarization-independent. The transmittance of the band is as high as 90–95%. The transmittance was calculated using a reference aluminum (Al) mirror instead of L1 and R1. For

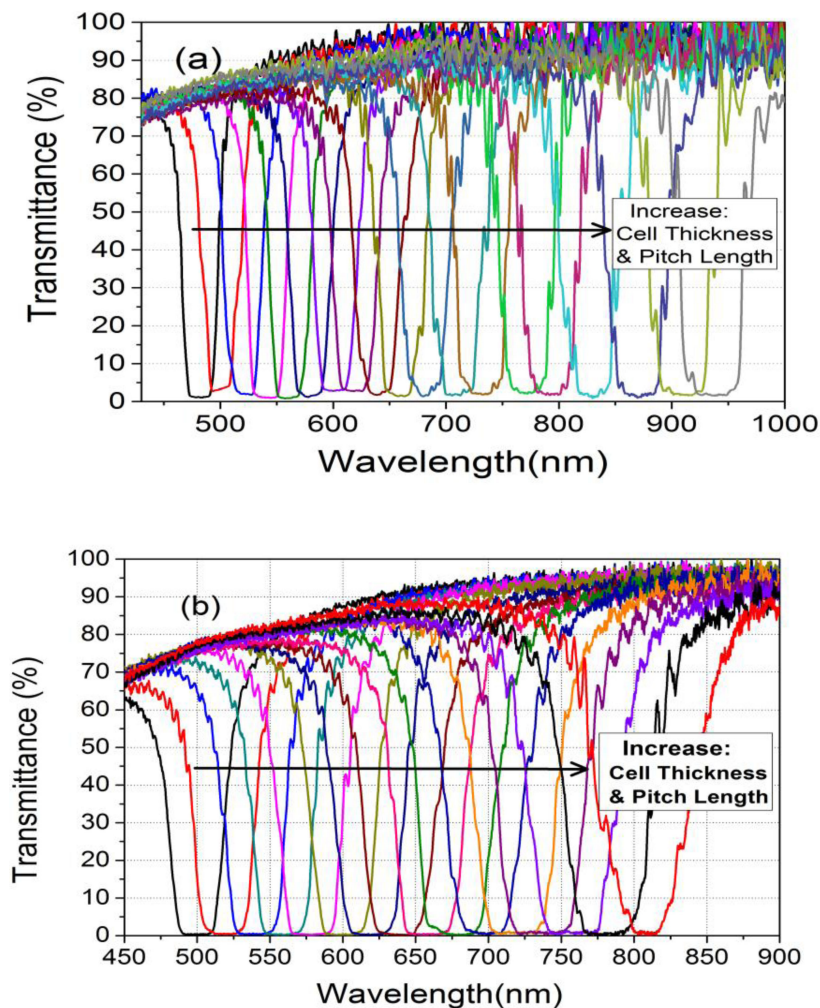


Fig. 6. Spectra of the continuous tunable notch filter system. (a) N1 filter system consisting of an L-CLC cell, an R-CLC cell, and W1. (b) N2 filter system consisting of two L-CLC cells, two R-CLC cells, and W1. The data were measured by spatially moving each CLC cells with translation stages to maintain the same PBG position. The data were shown in a low density to easily distinguish one by one.

all wavelengths, the transmittance was corrected by the Al mirror data provided by the Edmund Optics Co. (USA): reflectance $\sim 95\%$ from 450 nm to 650 nm, minimum value $\sim 85\%$ near 870 nm. Although the AR-layer on BK7 greatly improved notch and band-pass filter efficiency, some light leakage still occurred outside the photonic band, $\sim 8\%$ near 500 nm; as the wavelength increased the leakage decreased to 1% near 900 nm.

On the other hand, filter bandwidth is an important parameter for practical application. The FWHM of the band-pass filter spectrum near 475 nm was ~ 30 nm and increased to ~ 60 nm near 860 nm. This behavior is an intrinsic property of the CLC materials. However, this intrinsic behavior could be changed somewhat by combining some CLC devices. By employing the BS, L1, R1', and W2 in Fig. 5, the bandwidth of the band-pass filter was actively controlled. The principle is as follows; when a collimated unpolarized light passes through the BS and then incident to the position of the L1, the PBG of which is located between 600 and 640 nm, left circularly polarized light in the PBG is reflected to the BS. The light in the PBG is then reflected again to R1' at the BS, where its polarization state is changed from left to right circularly polarized light. Meanwhile, the PBG position of R1' is moved to between 610 nm and 650 nm. The right circularly polarized light in the PBG of the incident light between 610 nm and 640 nm is reflected at R1', and only the right

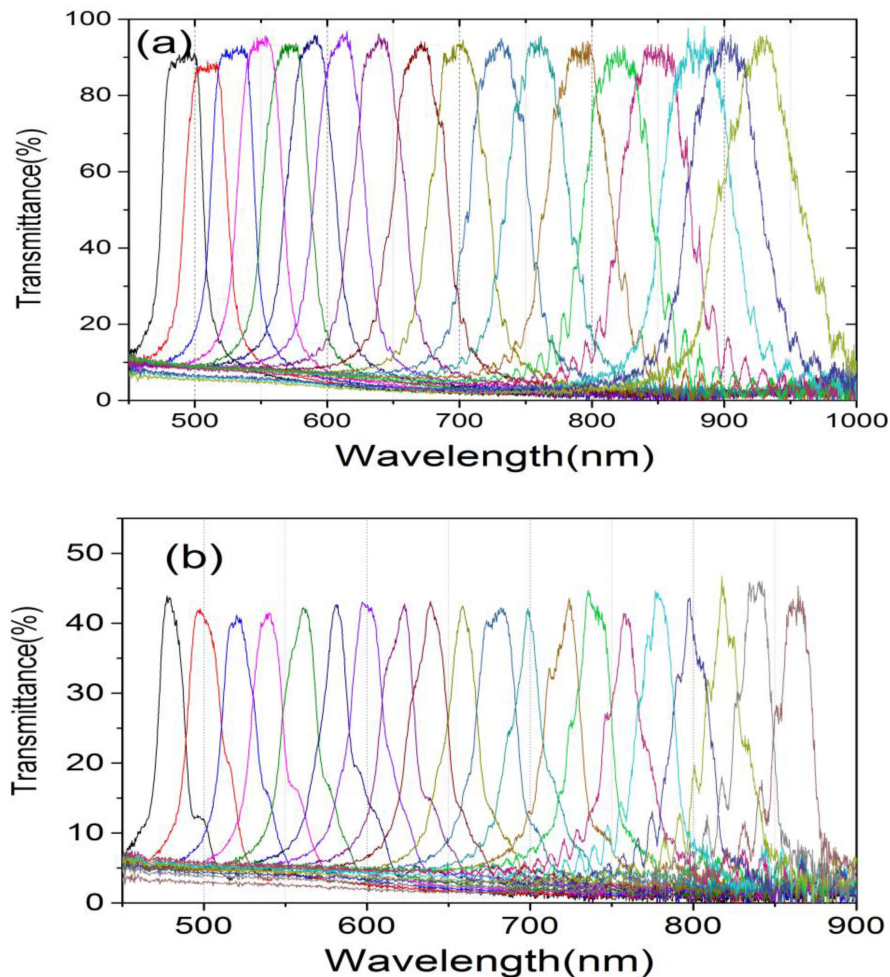


Fig. 7. (a) Spectra from the continuous tunable band-pass filter system. (b) Bandwidth reduced spectra from the original broad bandwidth to ~ 18 nm. The data were measured by spatially moving each CLC cells with translation stages to maintain the same PBG position. The data were shown in a low density to easily distinguish one by one.

circularly polarized light between 600 nm and 610 nm passes through R1' because it is an R-CLC. Therefore, the bandwidth could be decreased from 40 nm to 10 nm, and the bandwidth of the band-pass filter system could be reversibly controlled from ~ 10 nm to 40 nm by moving the PBG position of R1'. As the bandwidth decreases, the peak intensity can decrease. The cell position of L1 and R1' could be changed to change the polarization state of the transmitted light from right to left circular polarization. Fig. 7(b) shows band-pass filter spectra from ~ 475 nm to ~ 880 nm in which the FWHM is decreased from the original bandwidth of 33 nm \sim 60 nm to 16 nm \sim 25 nm by moving the PBG position of R1'. The peak intensity of the band-pass filter is the transmission rate for incident light. Via fine movement of the PBG position of L1 and R1', the band could also be finely shifted. With a refractive index mismatch at the boundary between layers in the cell, there is transmittance outside the band of $\sim 3\%$ near 500 nm. The switching speed of the devices only depends on the mechanical movement of the translation stages.

5. Conclusion

We studied continuous wavelength tunable and bandwidth variable optical notch and band-pass filters and their optical characteristics. Our strategy was to combine four pieces of left- and right-

handed circular CLC cells and to introduce an anti-reflection layer on the filter device, greatly improving filter performance. The filter comprised CLC wedge cells with a continuous pitch gradient without extra optical components such as polarizers and retarders; the band wavelength position of the notch/band-pass filters were spatially tuned from 470 nm to 1000 nm. Notch filters are polarization-independent in the spectral ranges. The band-pass filters could be polarization-dependent or polarization-independent based on the cell alignment. Furthermore, the bandwidth could be reversibly varied from the original bandwidth of ~ 60 nm to ~ 18 nm. No light leakage was observed inside the band, and outside the band transmittance was up to 70~100%. Our optical tunable filter strategies could be useful for wavelength tunable spectroscopic instruments, such as Raman spectroscopy, life science devices, optical communication systems, supercontinuum system, and astronomical telescopes, among others. The switching speed of the devices only depends on the mechanical movement of the translation stages.

Acknowledgment

The authors would like to thank Y.-K. Yun at Merck Ltd. Korea for supplying MLS-6608, R811, and S811, and S.-M. Park at Nissan Chemical Korea Co. Ltd. for supplying polyimide (SE-5291).

References

- [1] L. W. Luo *et al.*, "WDM-compatible mode-division multiplexing on a silicon chip," *Nature Commun.*, vol. 5, pp. 1–7, 2014.
- [2] A. J. Lowery, J. Schröder, and L. B. Du, "Flexible all-optical frequency allocation of OFDM subcarriers," *Opt. Exp.*, vol. 22, no. 1, pp. 1045–1057, 2014.
- [3] J. P. J. H. Zang and B. Mukherjee, "A review of routing and wavelength assignment approaches for wavelength-routed optical WDM networks," *Opt. Netw. Mag.*, pp. 47–60, Jan. 2000.
- [4] Bo Dai *et al.*, "Optical bandpass/notch filter with independent tuning of wavelength and bandwidth based on a blazed diffraction grating," *Opt. Exp.*, vol. 22, no. 17, pp. 20284–20291, 2014.
- [5] Z. S. Shen, H. Hasegawa, K. Sato, T. Tanaka, and A. Hirano, "A novel elastic optical path network that utilizes bitrate-specific anchored frequency slot arrangement," *Opt. Exp.*, vol. 22, no. 3, pp. 3169–3179, 2014.
- [6] M. Jinno *et al.*, "Distance-adaptive spectrum resource allocation in spectrum-sliced elastic optical path network," *IEEE Comm. Mag.*, vol. 48, no. 8, pp. 138–145, Aug. 2010.
- [7] J. W. Jeong, I. W. Jung, H. J. Jung, D. M. Baney, and O. Solgaard, "Multifunctional tunable optical filter using MEMS spatial light modulator," *J. Microelectromech. Syst.*, vol. 19, no. 3, pp. 610–618, 2010.
- [8] J. Stone and L. W. Stulz, "Pigtailed high-finesse tunable fibre fabry-perot interferometers with laser, medium and small free spectral ranges," *Electron. Lett.*, vol. 23, no. 15, pp. 781–783, 1987.
- [9] E. B. Dan Sadot, "Tunable optical filters for dense WDM networks," *IEEE Commun. Mag.*, vol. 36, no. 12, pp. 50–55, Dec. 1998.
- [10] N. E. Oton E, "Wide tunable shift of the reflection band in dual frequency cholesteric liquid crystals," *Opt. Exp.*, vol. 25, no. 11, pp. 13314–13323, 2017.
- [11] S. Fan, P. R. Villeneuve, and J. D. Joannopoulos, "Large omnidirectional band gaps in metallodielectric photonic crystals," *Phys. Rev. B*, vol. 54, pp. 11245–11251, 1996.
- [12] C. Tserkezis, "Effective parameters for periodic photonic structures of resonant elements," *J. Phys., Condens. Matter*, vol. 21, 2009, Art. no. 155404.
- [13] C. Tserkezis, N. Stefanou, G. Gantzounis, and N. Papanikolaou, "Photonic surface states in plasmonic crystals of metallic nanoshells," *Phys. Rev. B*, vol. 84, 2011, Art. no. 115455.
- [14] H.-F. Zhang, "Investigations on the two-dimensional aperiodic plasma photonic crystals with fractal Fibonacci sequence," *AIP Adv.*, vol. 7, 2017, Art. no. 075102.
- [15] H. R. Morris, C. C. Hoyt, and P. J. Treado, "Imaging spectrometers for fluorescence and raman microscopy: Acousto-Optic and liquid crystal tunable filters," *Appl. Spectrosc.* vol. 48, no. 7, pp. 857–866, 1994.
- [16] I. A. Ofir Aharon, "Design of wide band tunable birefringent filters with liquid crystals," *PIERS ONLINE*, vol. 5, no. 6, pp. 555–560, 2009.
- [17] L. JD *et al.*, "Spatially tunable photonic bandgap of wide spectral range and lasing emission based on a blue phase wedge cell," *Opt. Exp.*, vol. 22, no. 14, pp. 1658–1662, 2014.
- [18] Y. Huang, M. Jin, and S. Zhang, "Polarization-independent bandwidth-variable tunable optical filter based on cholesteric liquid crystals," *Japanese J. Appl. Phys.*, vol. 53, 2014, Art. no. 072601.
- [19] A. Ogiwara and H. Kakiuchida, "Thermally tunable light filter composed of cholesteric liquid crystals with different temperature dependence," *Sol. Energy Mater. Sol. Cells*, vol. 157, pp. 250–258, 2016.
- [20] A. Y. Fuh, S. J. Ho, S. T. Wu, and M. S. Li, "Optical filter with tunable wavelength and bandwidth based on phototunable cholesteric liquid crystals," *Appl. Opt.*, vol. 53, pp. 1658–1662, 2014.
- [21] S. Reichel, U. Brauneck, S. Bourquin, and A. Marín-Franch, "Narrow bandpass steep edge optical filter for the JAST/T80 telescope instrumentation," *SPIE, Opt. Eng. Appl.*, vol. 8860, pp. 88600M-1–88600M-12, 2013.

- [22] E. Nicolescu and M. J. Escuti, "Polarization-independent tunable optical filters based on liquid crystal polarization gratings," *Appl. Opt.*, vol. 49, no. 20, pp. 3900–3904, 2010.
- [23] M.-Y. Jeong and J. Y. Mang, "Continuously tunable optical notch filter and band-pass filter systems that cover the visible to near-infrared spectral ranges," *Appl. Opt.*, vol. 57, no. 8, pp. 1962–1966, 2018.
- [24] O. Aharon and I. Abdulhalim, "Liquid crystal Lyot tunable filter with extended free spectral range," *Opt. Exp.*, vol. 17, no. 14, pp. 11426–11433, 2009.
- [25] S. Isaacs, F. Placido, and I. Abdulhalim, "Investigation of liquid crystal Fabry–Perot tunable filters: Design, fabrication, and polarization independence," *App. Opt.*, vol. 53, no. 29, pp. H91–H101, 2014.
- [26] M. Abuleil and I. Abdulhalim, "Narrowband multispectral liquid crystal tunable filter," *Opt. Lett.* vol. 41, no. 9, pp. 1957–1960, 2016.
- [27] M.-Y. Jeong and J. W. Wu, "Continuous spatial tuning of laser emissions with tuning resolution less than 1 nm in a wedge cell of dye-doped cholesteric liquid crystals," *Opt. Exp.*, vol. 18, pp. 24221–24228, 2010.
- [28] M. Y. Jeong and J. Cha, "Firsthand in situ observation of active fine laser tuning by combining a temperature gradient and a CLC wedge cell structure," *Opt. Exp.*, vol. 23, pp. 21243–21253, 2015.
- [29] K. Sato, K. Mizutani, S. Sudo, K. Tsuruoka, K. Naniwae, and K. Kudo, "Wideband external cavity wavelength-tunable laser utilizing a liquid-crystal-based mirror and an intracavity etalon," *J. Lightw. Technol.*, vol. 25, no. 8, pp. 2226–2232, Aug. 2007.
- [30] M.-Y. Jeong and J. W. Wu, "Temporally stable and continuously tunable laser device fabricated using polymerized cholesteric liquid crystals," *Japanese J. Appl. Phys.*, vol. 51, 2012, Art. no. 082702.
- [31] O. Castany, L. Dupont, A. Shuaib, J. P. Gauthier, C. Levallois, and C. Paranthoen, "Tunable semiconductor vertical-cavity surface-emitting laser with an intracavity liquid crystal layer," *Appl. Phys. Lett.*, vol. 98, no. 16, 2011, Art. no. 161105.
- [32] V. Joshi, K.-H. Chang, D. A. Paterson, J. M. D. Storey, C. T. Imrie, and L.-C. Chien, "Fast flexoelectro-optic response of bimesogen-doped polymer stabilized cholesteric liquid crystals in vertical standing helix mode," *SID Digest*, vol. 4, pp. 1849–1852, 2017.
- [33] Y. Li, D. Luo, and Z. H. Peng, "Full-color reflective display based on narrow bandwidth templated cholesteric liquid crystal film," *Opt. Mater. Exp.*, vol. 7, no. 1, pp. 16–24, 2017.
- [34] C. Levallois *et al.*, "Liquid crystal-based tunable photodetector operating in the telecom C-band," *Opt. Exp.*, vol. 26, no. 20, pp. 25952–25961, 2018.
- [35] Y. Huang, L.-P. Chen, C. Doyle, Y. Zhou, and S.-T. Wu, "Spatially tunable laser emission in dye-doped cholesteric polymer films," *Appl. Phys. Lett.*, vol. 89, 2006, Art. no. 111106.
- [36] B. Kang, H. Choi, M. Jeong, and J. W. Wu, "Effective medium analysis for optical control of laser tuning in a mixture of azo-nematics and cholesteric liquid crystal," *J. Opt. Soc. Amer. B*, vol. 27, no. 2, pp. 204–207, 2010.
- [37] H. Yu, B. Y. Tang, J. Li, and L. Li, "Electrically tunable lasers made from electro-optically active photonics band gap materials," *Opt. Exp.*, vol. 13, no. 18, pp. 7243–7249, 2005.
- [38] P. G. De Gennes and J. Prost, *The Physics of Liquid Crystals*. Oxford, U.K.: Clarendon, 1993, ch. 6.
- [39] M.-Y. Jeong and J. W. Wu, "Continuous spatial tuning of laser emissions in a full visible spectral range," *Int. J. Mol. Sci.*, vol. 12, pp. 2007–2018, 2011.
- [40] Q. Hong, T. X. Wu, and S.-T. Wu, "Optical wave propagation in a cholesteric liquid crystal using the finite element method," *Liquid Crystals*, vol. 30, no. 3, pp. 367–375, 2003.
- [41] D. W. Berreman, "Optics in stratified and anisotropic media: 4×4 matrix formulation," *J. Opt. Soc. Amer.*, vol. 62, pp. 502–510, 1972.
- [42] D. W. Berreman, "Optics in smoothly varying anisotropic planar structures: Application to liquid crystal twist cells," *J. Opt. Soc. Amer.*, vol. 63, pp. 1374–1380, 1973.